



HAL
open science

Study of electrical double layer effect on chloride transport in unsaturated concrete

Phu Tho Nguyen, Ouali Amiri

► **To cite this version:**

Phu Tho Nguyen, Ouali Amiri. Study of electrical double layer effect on chloride transport in unsaturated concrete. *Construction and Building Materials*, 2014, 50, pp.492-498. 10.1016/j.conbuildmat.2013.09.013 . hal-03286594

HAL Id: hal-03286594

<https://hal.science/hal-03286594>

Submitted on 28 Jul 2021

HAL is a multi-disciplinary open access archive for the deposit and dissemination of scientific research documents, whether they are published or not. The documents may come from teaching and research institutions in France or abroad, or from public or private research centers.

L'archive ouverte pluridisciplinaire **HAL**, est destinée au dépôt et à la diffusion de documents scientifiques de niveau recherche, publiés ou non, émanant des établissements d'enseignement et de recherche français ou étrangers, des laboratoires publics ou privés.



Distributed under a Creative Commons Attribution 4.0 International License

Study of electrical double layer effect on chloride transport in unsaturated concrete

P.T. Nguyen ^a, O. Amiri ^{a,b,*}

^a LaSIE FRE-CNRS 3474, Université de La Rochelle, Pole Sciences et Technologie, Avenue Michel Crépeau, 17042 La Rochelle, France

^b Institut de Recherche en Génie Civil et Mécanique (GeM), UMR-CNRS 6183, Université de Nantes (IUT de Saint Nazaire), 58 rue Michel Ange, 44600 Saint Nazaire, France

In this paper, a physical model of chloride ingress concretes is proposed. The originality of the model lies in its consideration of electrical double layer (EDL) phenomenon in unsaturated concrete. The EDL is occurring at the interface between pore walls and pore solution. The work is performed by solving the multispecies ionic transport equations coupled with those of humidity. To show the effect of slag and fly ash, several concretes were considered. The chloride profile was simulated. The results show that chloride concentration increase for EDL negative more than EDL positive. The EDL effect is reduced in unsaturated concrete due to discontinuity of liquid phase. Finally, it is also shown that the concrete containing slag develops and EDL more important than those manufactured with fly ash.

1. Introduction

The corrosion of steel reinforcement is one of the most important causes of degradation of concrete structures. The corrosion is due to chloride ingress mainly in the coast zones. In fact, when the chloride concentration reaches the threshold value, the corrosion of steel began until the local ruin of the structure according to TUTTI model [1,2]. Consequently, the service life of the structures is reduced.

To predict correctly the service life, it is important to take into account in the chloride transfer model, the main chemical and physical phenomena's occurring in cement based materials such the chemical binding, the activity of pore solution, the electrostatic interaction between the ions contained in the pore solution and the electrical double layer (EDL).

Several models have been developed during the two last decades. Some models are monospecies, based on modified Fick's law [3–5] have just taken into account the chemical binding of chloride through the isotherm (Freundlich or Langmuir). Other models [6,7] considered as “multispecies” are based on Nernst-Planck equation. These models are more consistent, because in addition to chloride chemical binding they take into account some physical phenomena mainly the interaction between chloride and other ions contained in the pore solution of concrete and electrocapillary process occurring between the pores walls and the pore solution. This process known under “electrical double layer (EDL)” induces a viscous electric effect which slowed the chloride ingress [7]. Also, in other fields such nanofiltration membranes and clays, the EDL takes a significant role in the transport of ions.

In the field of cement based materials, Chatterji and Kawamura [8] were the first who studied the EDL effect on ionic transport, but qualitatively. We can also note the several studies of Nägele [9–15] which deal only with the measurement of zeta potential considered as the main parameter of EDL. But to our knowledge, the studies dealing with the EDL effect on chloride transport from qualitative point of view, mainly in unsaturated concrete, are few. So the

* Corresponding author at: Institut de Recherche en Génie Civil et Mécanique (GeM), UMR-CNRS 6183, Université de Nantes (IUT de Saint Nazaire), 58 rue Michel Ange, 44600 Saint Nazaire, France. Tel.: +33 (0)2 02 72 64 87 36.

E-mail address: ouali.amiri@univ-nantes.fr (O. Amiri).

goal of this work is to highlight the EDL effect in unsaturated concrete submitted to chloride ingress. To reach this aim, we have to combine ions and humidity transport with the EDL effect at macroscopic scale stems from Poisson–Boltzmann equation. Simulation of chlorides profiles in concretes containing fly ash and slag were carried out to show the effect of the sign of EDL on chloride ingress.

2. Electrical double layer (EDL) phenomenon: brief description

In order to understand the EDL effect, we just give a brief description of this phenomenon. More details are given in [7].

The Stern model (Fig. 1) is generally adopted to describe EDL phenomenon. At the interface between the pore walls (cement matrix) and the pore solution, ions are physically adsorbed by Van der Waals ‘forces. An imbalance ionic is then established, but the bulk remains in equilibrium.

The interface is structured in two parts, a compact (Helmholtz) layer ($x \leq x_2$) and a diffuse layer (from x_2 to the bulk): the two parts constitutes the electrical double layer. The compact layer ($x \leq x_2$) is made of solvated ions, adsorbed at the surface. The potential in the EDL due to the imbalance ionic follows to the Poisson equation. At the compact layer, the potential is known as “zeta potential” and can be measured by a zeta meter. The extension of the potential is occurred on a distance called “Debye length” which depends on the temperature, the ionic concentration of the bulk solution and its dielectric permittivity. In this paper, we consider that a pore of a porous medium can be schematically represented by two parallel flat plates distant from d which is considered as the pore diameter. In this case, two diffuse layers are in face to face which can overlap when the pore diameter is close to Debye length.

3. Physical modeling

3.1. Ionic transfer

In saturated medium the water movement by advection is dramatically low according to the permeability of concrete. In the unsaturated one, convection phenomena play an important role in the transfer of ions, especially in the humidification phase. By analyzing the electrochemical potential at the microscopic level, some authors [17–20] have shown that the consideration of the EDL effect leads to a change on flux of ions in cement based materials. Indeed, in the small pores size (including gel pores), electrostatic interactions occur through the EDL phenomenon between

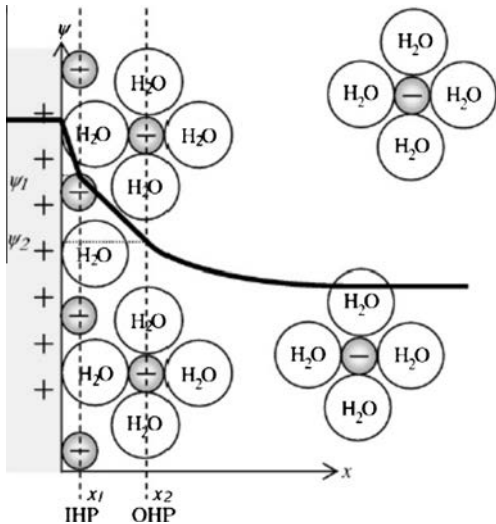


Fig. 1. Schematic view of the EDL [16].

the surface of the cement matrix and the ions contained in the pore solution. Therefore, the ion concentration is not homogeneous locally. Under these conditions, the ion flux usually based on the Nernst–Planck equation is modified [21,22]. The modification concerns the concentration of anions and cations:

$$\bar{C}_i = K_{\mp} C_i \quad (1)$$

where K_+ and K_- are two coefficients which traduce EDL effect on cation and anion fluxes, respectively. C_i is the average concentration of specie i .

By taking into account equation, the classical equation of Nernst–Planck extended to unsaturated transport, becomes:

$$\frac{\partial(wK_{\mp}C_i)}{\partial t} + (1 - \varepsilon_0) \frac{\partial(K_{\mp}C_{ib})}{\partial t} - \text{div} \left(\underbrace{wD_iK_{\mp}\text{grad}C_i}_{\text{diffusion}} + \underbrace{\frac{K_{\mp}D_iFz_i}{RT}C_iw\text{grad}\Psi}_{\text{migration}} - \underbrace{K_{\mp}wC_iU}_{\text{convection}} \right) = 0 \quad (2)$$

with ε_0 is the porosity of the material, w is water content. C_i is the concentration of chemical specie i contained in the pore solution. C_{ib} is the concentration of specie i bound to cement matrix of the concrete. ψ is the electrical potential in the pore solution. D_i is the diffusion coefficient of the specie i and z_i is its valence. F is the Faraday’s constant, R is the gas constant and T is the thermodynamic temperature (293 °K).

In the pore solution, the ions interact with each other, producing an electrostatic potential ψ which can be deduced from Eq. (2) in the case of a natural diffusion (no current density):

$$\text{grad}\Psi = - \frac{\sum_{i=1}^n D_i K_{\mp} C_i z_i w \text{grad} C_i - \sum_{i=1}^n z_i w U K_{\mp} C_i}{\frac{F}{RT} \sum_{i=1}^n D_i K_{\mp} C_{ib} z_i^2 w \nabla C_{ib}} \quad (3)$$

$$K_+ = \frac{A(\kappa d)^2}{1 - AB\kappa d + A(\kappa d)^2} + \frac{1 + Z}{2} \frac{2q}{FdC_{pc}} \quad (4)$$

$$K_- = K_+ - \frac{2q}{FdC_{pc}} \quad (5)$$

A and B are two parameters which depend on the zeta potential and the pore diameter d , the concentration of the bulk C_{pc} , the surface density charge q and on Debye constant κ [7], Z is the sign of the EDL ($Z = 1$, EDL positive; $Z = -1$, EDL negative).

The rate of chemical chloride binding considered follows the Langmuir isotherm.

$$C_{ib} = \frac{aK_{\mp}C_i}{1 + bK_{\mp}C_i} \quad (6)$$

The constants a and b are defined in the Section 4.

3.2. Humidity transfer

The mains assumptions considered are:

- The liquid phase is constituted by water. The gas one contains dry air and steam. The pressures in these two phases are noted p_a and p_v , respectively.
- The gravity effect is negligible.

The balance equations are for each phase liquid (w) (water vapor) and air (a) are:

$$\frac{\partial[\rho_w w]}{\partial t} = -\text{div}(\rho_w v_w) - \dot{m} \quad (7)$$

$$\frac{\partial[\rho_v(\varepsilon_0 - w)]}{\partial t} = -\text{div}(D_{va}\text{grad}(\rho_v)) + \dot{m} \quad (8)$$

$$\frac{\partial[\rho_a(\varepsilon_0 - w)]}{\partial t} = -\text{div}(D_{va}\text{grad}(\rho_a)) \quad (9)$$

where ρ_w , ρ_v and ρ_a are the densities of water, steam and air respectively. \dot{m} is the evaporation (or condensation) ratio at the interface liquid–gas. Eqs. (10) and (11) give the velocity of liquid phase and the capillary pressure.

$$v_w = -\frac{K_l K_{rl}}{\mu_l} \text{grad}(P_l) \quad (10)$$

$$P_c = P_g - P_l \quad (11)$$

For capillary pressure calculation, we consider GAB model, modified and adapted for cement based materials, in previous studies [23,24]:

$$P_c = -\frac{\rho_w RT}{M_w} \ln\left(\alpha_c + \frac{1}{2} \sqrt{\beta_c + \gamma_c \frac{\varepsilon_0}{w}}\right) \quad (12)$$

where ρ_w , M_w are the density and molar mass of water, respectively. α_c , β_c , γ_c are the parameters which depend on the material (see Table 3 in Section 4). The calculations of these parameters is detailed in [23,24].

K_1 , K_{r1} , μ_1 are the intrinsic permeability, relative permeability and the density of water, respectively.

D_{va} is the diffusion coefficient of vapor in concrete.

$$D_{va} = 2.17 \times 10^{-5} \left(\frac{T}{T_{ref}}\right)^{1.88} * f_{res} \quad (13)$$

T , T_{ref} are the temperature of the material and the reference one, respectively. f_{ref} is tortuosity factor which depend on the water content and porosity according to Milligton model [25].

The sum of Eqs. (7) and (8) gives the macroscopic humidity transport equation:

$$\frac{\partial w}{\partial t} - \text{div}(D_w \text{grad}(w)) = 0 \quad (14)$$

D_w is called hydrical diffusion coefficient de diffusion.

$$D_w = -\frac{K_l K_{rl}}{\mu_l} \frac{\partial P_c}{\partial x} + \frac{D_{va}}{\rho_w} \frac{\partial \rho_v}{\partial w} \quad (15)$$

For the relative permeability K_{rl} , we considered the Van Genechten model [26]

4. Numerical simulations: methodology of solving and output of the model

The model of ionic and humidity transport is described by the partial differential equations (2) and (13). These equations are solved numerically in the one-dimensional case by using volume

Table 1
Materials used.

Concrete	CR	BFS30	BFS75	FA30
Gravel 6/10 (kg/m ³)	1012.7	1077.37	1037.07	1048.19
Sand (0/4) (kg/m ³)	855	848.26	816.48	824.46
CEM I 52.5 (kg/m ³)	330	218.66	102.84	241.07
Slag (kg/m ³)	–	93.71	309.58	–
Fly ash (kg/m ³)	–	–	–	103.30
Water (kg/m ³)	198	181	170	182.12
W/C	0.6	0.63	0.44	0.57
d (nm)	95.6	21.1	3	120.7
Water porosity ε_0 (%)	15.9	17.5	14.3	16.5
Apparent density (kg/m ³)	2320	2260	2340	2280
Diffusion coefficient ($\times 10^{-12}$ m ² s ⁻¹)	12.9	7.2	2.3	6.4

finite method with explicit scheme. For the simulations, a cubic concrete sample with 5 cm of thickness is considered. Only one side is exposed to a saline solution (500 mol m⁻³, we try to simulate sea water). For the others sides, to simulate the multispecies pore solution of concrete, the concentrations of Cl⁻, OH⁻, Na⁺ and K⁺ considered as initial conditions are: respectively, 0 mol m⁻³, 108 mol m⁻³, 25 mol m⁻³ and 83 mol m⁻³.

To take into account the EDL effect, the concentrations are corrected par the coefficient K_{mp} previously defined.

$$\bar{C}_i(x=0, t) = K_{\pm}(x=0, t)C_i \quad (16)$$

4.1. Characteristics of the tested materials

The simulations of chloride profile were carried out 4 types of concrete: the concrete reference (CR) manufactured with ordinary cement (CEM I), 3 others concrete where the ordinary cement is substituted by 30% (BFS30) and 75% (BFS75) of blast furnace slag and by 30% of fly ash (FA30). The mains characteristics of these concretes are summarized in Table 1. The water permeability is difficult to obtain experimentally. As first step, we considered the value proposed ($K_l = 5 \times 10^{-21}$ (m²)) by Baroghel–Bounny [27] for the materials with an equivalent porosity to those of the concretes considered in this study.

We have to that note that the chloride diffusion coefficient given in Table 1, is determined by diffusion test with the method of chronoamperometry [7,22,16]. The water porosity is measured according to AFREM recommendations [28]. d is the percolation diameter determined by mercury intrusion porosimetry (MIP) [29–32]. Fig. 2 gives the pore size distribution (PoD) of the tested concretes.

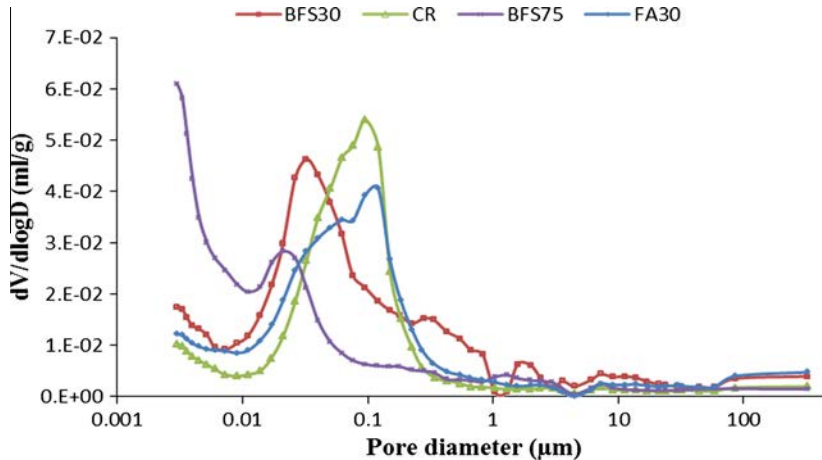


Fig. 2. Pore size distribution of the concretes.

The parameters a and b of Langmuir isotherm are determined by the test of isotherm of interaction according to AFREM recommendations [28]. The values are given in Table 2. We suppose that all other ions are not absorbed in the concrete.

As it is shown in Fig. 2, the PoD of the tested materials is globally monomodal. The effect of slag is to reduce the size of the pores more than the fly ash. As it is shown in the next section, the size of pore is linked to electrical double layer effect.

For the humidity transport, we have used the GAB isotherm needed for the capillary pressure calculation. Table 3 gives the main parameters of this isotherm for each concrete.

Table 2
Parameters of langmuir isotherm for chloride binding.

Concrete	$a \left(\frac{\text{m}^3 \text{ solution}}{\text{kg concrete}} \right) 10^{-4}$	$b \left(\frac{\text{m}^3 \text{ solution}}{\text{mol}} \right) 10^{-4}$
CR	3.88	20.3
BFS30	2.42	8.86
BFS75	1.28	4.36
FA30	1.87	7.21

Table 3
GAB parameters for the tested concretes.

Materials	α_c	β_c	γ_c
CR	-6.00	182.33	97.73
BFS30	-6.00	182.33	88.95
BFS75	-5.43	149.33	73.30
FA30	-5.89	175.76	68.64

4.2. Chlorides profiles simulations and discussion

To simulate the electrical double layer effect, we have simulated the chloride profile for both saturated and unsaturated concretes for 1 year. For the unsaturated conditions, the drying and wetting cycle considered is 18 H and 6 H, respectively. 3 cases of electrical double layer were considered: positive EDL (zeta potential = +50 mV), EDL Negative (zeta potential = -50 mV) and without EDL effect. The result of the simulation is shown in the Figs. 3-6.

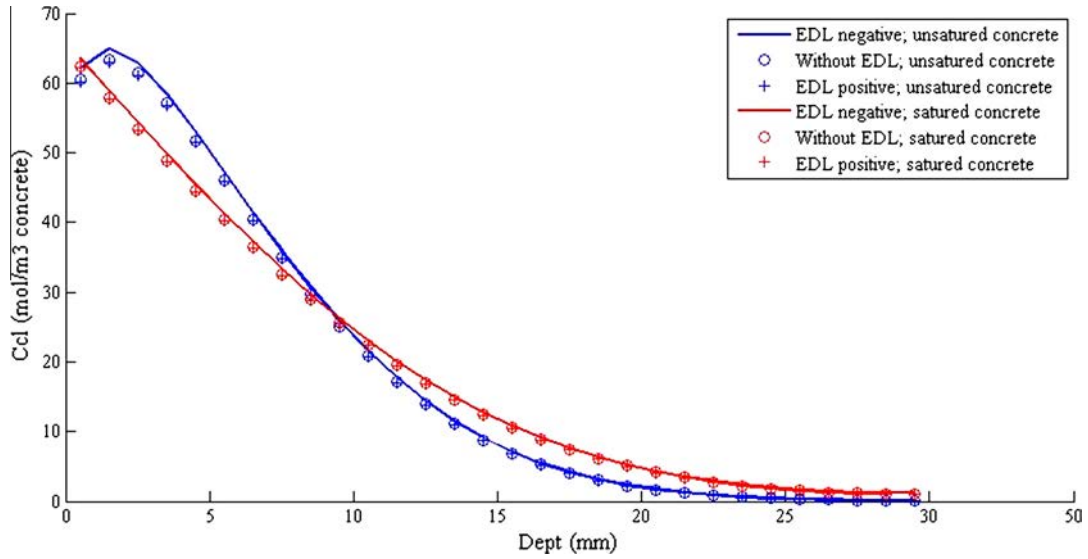


Fig. 3. Chloride profile of concrete reference CR.

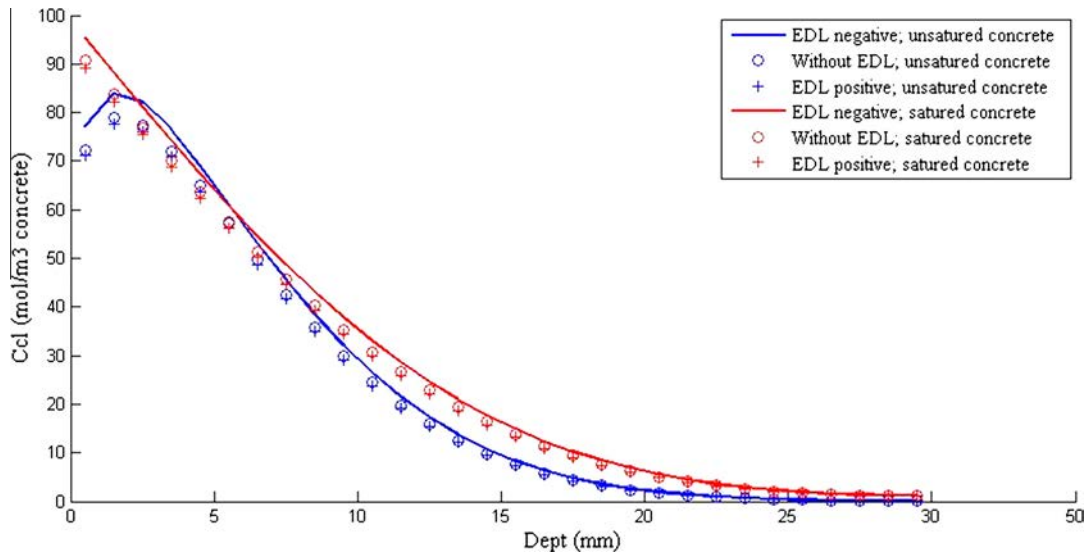


Fig. 4. Chloride profile of concrete BFS30.

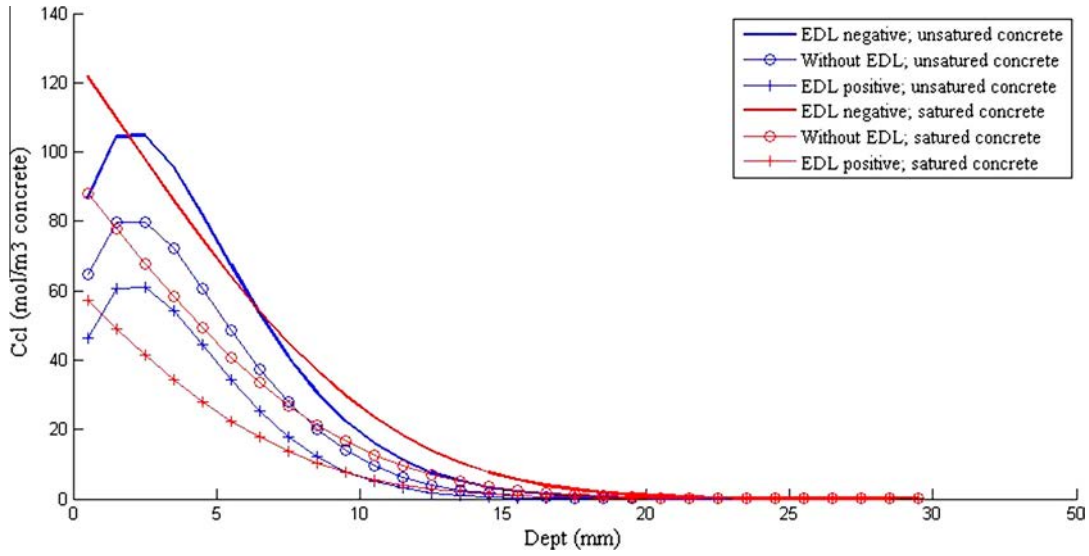


Fig. 5. Chloride profile of concrete BFS75.

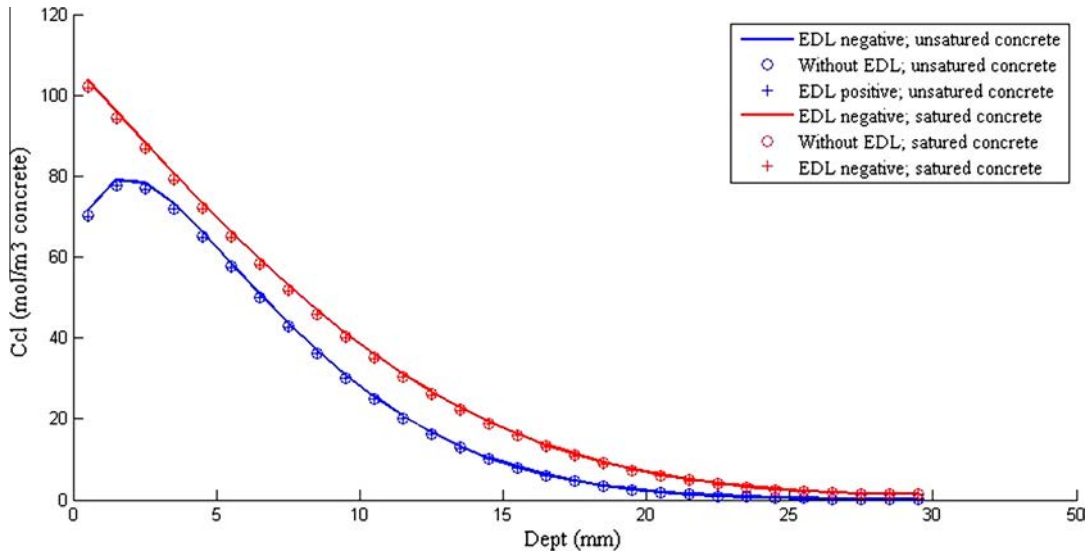


Fig. 6. Chloride profile of concrete FA30.

The first observation concern the EDL effect which is occurred when the concrete is saturated more than the unsaturated, because in the first case the liquid phase is continuous and the extension of EDL decrease mainly for the concrete containing slag. In fact, the cement matrix is negatively charged and the slag charged positively. Thus, the ionic strength and the EDL effect increase. This leads to an increasing of chloride concentration due the overlapping of EDL which occurs essentially in the concrete BFS75 due to the pore size (Fig. 5). The simulations show also the overlapping is greater when the zeta potential is negative.

4.3. Sensitivity of the model

The two main parameters of the EDL is the zeta potential and pore size. To show the sensitivity of the model according these two parameters, we simulated the profile of chloride ions for 3 values of zeta potential and pore diameters. Fig. 7 shows that chloride

concentration is inversely proportional ions to pore diameter. The EDL effect is greater when the pore diameter is close to Debye length (3 nm). Any variation of the pore size leads to a significant change of chloride concentration. This is explains the weak effect of EDL for the concretes CR, BFS30.

Concerning the zeta potential effect, Fig. 8 shows that the chloride profile is increased according to zeta potential. This is due to the fact that the overlapping of EDL within a pore is related to the intensity of physical adsorption which is strongly linked to the zeta potential.

The figure represents the sensibility of the model to the water permeability which is the main parameter governing the humidity transport. We note that the slightest variation of K_l of induced a modification in chloride profile. This result confirm that the prediction of chloride ingress in unsaturated concrete needs a model which combine both chloride and humidity transport and not Fick's laws (see Fig. 9).

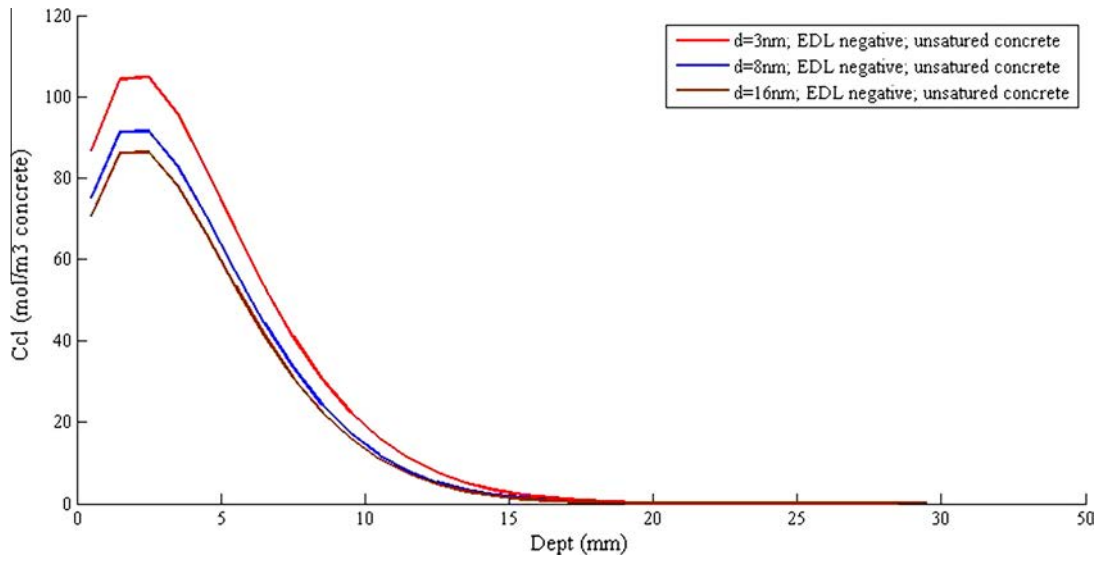


Fig. 7. Influence of size pore on chloride profile in the concrete BFS75.

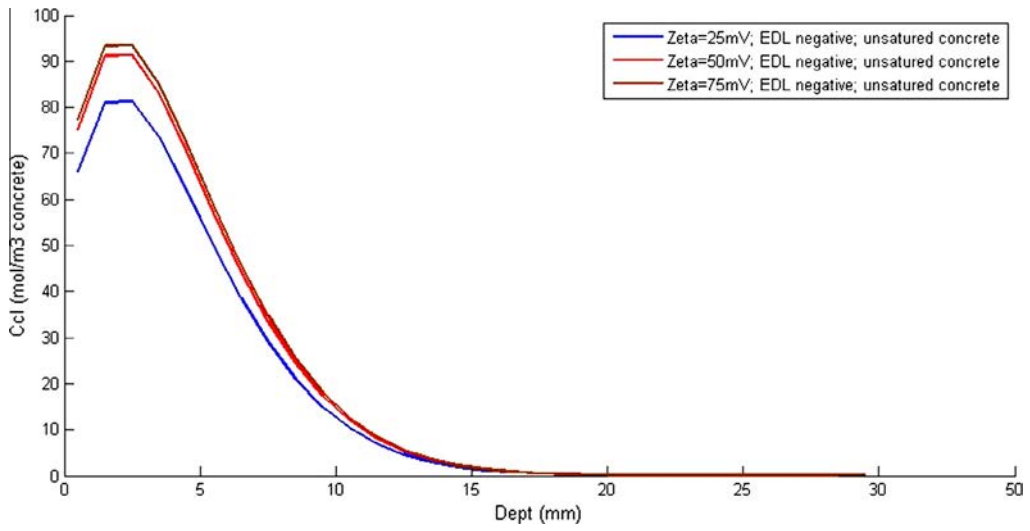


Fig. 8. Influence of zeta potential on chloride profile in the concrete BFS75.

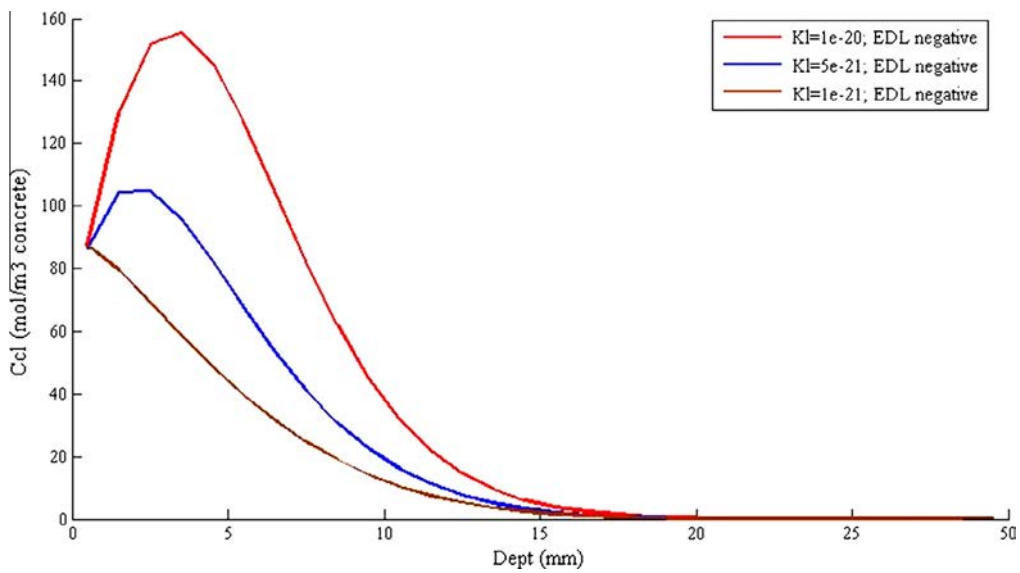


Fig. 9. Influence of water permeability of concrete on chloride profile in the concrete BFS75.

5. Conclusion

In this paper, the Electrical double layer (EDL) effect on chloride transport in the case of unsaturated concretes is studied. The main conclusions that we can draw are:

- The EDL effect is more significant in the saturated concrete than the unsaturated one, due to the continuity of liquid phase. But if the drying is strong (high permeability), the chloride concentration increase.
- The sign of EDL affect the chloride concentration which is increased when zeta potential is negative and decreased in the opposite case.
- The EDL effect is stronger in the concrete containing slag more than those manufactured with fly ash. This is due to the ferrous ions of slag which increase the ionic strength of the pore solution.
- The chloride concentration is linked the two parameters of electrical double layer zeta potential and pore diameter but below Debye length, the EDL effect becomes insignificant.

References

- [1] Clifton JR. Predicting the service life of concrete. *ACI Mater J* 1993;6(6):611–7.
- [2] Sobhani J, Ramezani-pour AA. Chloride-induced corrosion of RC structures. *Asian J Civ Eng Build Hous* 2007;8(5):531–47.
- [3] Tang L, Nilsson LO. Chloride binding capacity and binding isotherms of OPC pastes and mortars. *Cem Concr Res* 1993;23(2):247–53.
- [4] Pérez BM. Service life modelling of R.C. highway structures exposed to chlorides. University of Toronto; 1999.
- [5] Nielsen EP, Geiker MR. Chloride diffusion in partially saturated cementitious material. *Cem Concr Res* 2003;33(1):133–8.
- [6] Samson E, Marchand J. Modeling the transport of ions in unsaturated cement-based materials. *Comput Struct* 2007;85(23–24):1740–56.
- [7] Friedmann H, Amiri O, Ait-Mokhtar A, Dumargue P. A direct method for determining chloride diffusion coefficient by using migration test. *Cem Concr Res* 2004;34(11):1967–73.
- [8] Chatterji S, Kawamura M. Electrical double layer, ion transport and reactions in hardened cement paste. *Cem Concr Res* 1992;22(5):774–82.
- [9] Nägele EW. The transient zeta potential of hydrating cement. *Chem Eng Sci* 1989;44(8):1637–45.
- [10] Nägele E, Schneider U. The zeta-potential of cement: Part IV. effect of simple salts. *Cem Concr Res* 1987;17(6):977–82.
- [11] Nägele E, Schneider U. The zeta-potential of blast furnace slag and fly ash. *Cem Concr Res* 1989;19(5):811–20.
- [12] Nägele E. The zeta-potential of cement. *Cem Concr Res* 1985;15(3):453–62.
- [13] Nägele E. The Zeta-potential of cement: Part II: Effect of pH-value. *Cem Concr Res* 1986;16(6):853–63.
- [14] Nägele E. The zeta-potential of cement: Part III: The non-equilibrium double layer on cement. *Cem Concr Res* 1987;17(4):573–80.
- [15] Nägele E, Schneider U. The zeta-potential of cement: Pt. V: Effect of surfactants. *Cem Concr Res* 1988;18(2):257–64.
- [16] Friedmann H. Modélisation multi-espèces de l'électrodiffusion instationnaire des ions chlorures dans les mortiers de ciment-Intégration de la double couche électrique. Université de La Rochelle; 2003.
- [17] Nguyen TQ. Modélisation physico-chimiques de la pénétration des ions chlorures dans les matériaux cimentaires. école nationale des ponts et chaussées; 2007.
- [18] Samson E, Marchand J, Beaudoin JJ. Describing ion diffusion mechanisms in cement-based materials using the homogenization technique. *Cem Concr Res* 1999;29(8):1341–5.
- [19] Pintauro PN, Verbrugge MW. The electric-potential profile in ion-exchange membrane pores. *J Membr Sci* 1989;44(2–3):197–212.
- [20] O'Shea P. Physical landscapes in biological membranes: physic-chemical terrains for spatio-temporal control of bimolecular interactions and behavior. *Phil Trans R Soc* 2005;575–88.
- [21] Friedmann H, Amiri O, Ait-Mokhtar A. Physical modeling of the electrical double layer effects on multispecies ions transport in cement-based materials. *Cem Concr Res* 2008;38(12):1394–400.
- [22] Friedmann H, Amiri O, Ait-Mokhtar A. Modelling of EDL effect on chloride migration in cement-based materials. *Mag Concr Res* 2012;64(10):909–17.
- [23] Xi Y, Bažant ZP. Modeling chloride penetration in saturated concrete. *J Mater Civ Eng* 1999;11(1):58–65.
- [24] Xi Y, Bažant ZP, Jennings HM. Moisture diffusion in cementitious materials Adsorption isotherms. *Adv Cem Based Mater* 1994;1(6):248–57.
- [25] Millington RJ, Quirk JP. Permeability of porous solids. *Trans Faraday Soc* 1961;57(0):1200–7.
- [26] Genuchten MV. A closed-form equation for predicting the hydraulic conductivity of unsaturated soils. *Soils Sci Am J* 1980;44:892–8.
- [27] Baroghel-Bouny V. Caractérisation des pâtes de ciment et des bétons; méthodes, analyse, interprétations. Edition du Laboratoire Central des Ponts et Chaussées; 1994.
- [28] AFPC-AFREM. Durabilité des bétons-méthodes recommandées pour la mesure des grandeurs associées à la durabilité; 1997.
- [29] Vočka R, Gallé C, Dubois M, Lovera P. Mercury intrusion porosimetry and hierarchical structure of cement pastes: theory and experiment. *Cem Concr Res* 2000;30(4):521–7.
- [30] Cook RA, Hover KC. Mercury porosimetry of hardened cement pastes. *Cem Concr Res* 1999;29(6):933–43.
- [31] León y León CA. New perspectives in mercury porosimetry. *Adv Colloid Interface Sci* 1998;76–77(0):341–72.
- [32] Ait-Mokhtar A, Amiri O, Dumargue P, Bouguerra A. On the applicability of washburn law: study of mercury and water flow properties in cement-based materials. *Mater Struct* 2004;37(2):107–13.